JOURNAL OF VIROLOGY, June 1994, p. 3955–3964
0022-538X/94/$04.00+0

Vol. 68, No. 6

Localization of Rotavirus VP4 Neutralization Epitopes Involved in Antibody-Induced Conformational Changes of Virus Structure

YONG-JIE ZHOU, JOHN W. BURNS,† YASUYUKI MORITA,‡ TOMOYUKI TANAKA,§ AND MARY K. ESTES*

Division of Molecular Virology, Baylor College of Medicine, Houston, Texas 77030

Received 23 August 1993/Accepted 16 March 1994

We previously characterized three neutralization-positive epitopes (NP1 [1a and 1b], NP2, and NP3) and three neutralization-negative epitopes on the simian rotavirus SA11 VP4 with 13 monoclonal antibodies (MAbs). Conformational changes occurred as a result of the binding of NP1 MAbs to the SA11 spike VP4, and enhanced binding of all neutralization-negative MAbs was observed when NP1 MAbs bound VP4 in a competitive MAb capture enzyme-linked immunosorbent assay. To further understand the structure and function of VP4, we have continued studies with these MAbs. Electron microscopic and sucrose gradient analyses of SA11-MAb complexes showed that triple-layered viral particles disassembled following treatment with NP1b MAbs 10G6 and 7G6 but not following treatment with NP1a MAb 9F6, NP2 MAb 2G4, and NP3 MAb 23. Virus infectivity was reduced approximately 3 to 5 logs by the NP1b MAbs. These results suggest that NP1b MAb neutralization occurs by a novel mechanism. We selected four neutralization escape mutants of SA11 with these VP4 MAbs and characterized them by using plaque reduction neutralization assays, hemagglutination inhibition assays, and an antigen capture enzyme-linked immunosorbent assay. These analyses support the previous assignment of the NP1a, NP1b, NP2, and NP3 MAbs into separate epitopes and confirmed that the viruses were truly neutralization escape mutants. Nucleotide sequence analyses found 1 amino acid (aa) substitution in VP8* of VP4 at (i) aa 136 for NP1a MAb mutant 9F6R, (ii) aa 180 and 183 for NP1b MAb mutants 7G6R and 10G6R, respectively, and (iii) aa 194 for NP3 MAb mutant 23R. The NP1b MAb mutants showed an unexpected enhanced binding with heterologous nonneutralization MAb to VP7 compared with parental SA11 and the other mutants. Taken together, these results suggest that the NP1b epitope is a critical site for VP4 and VP7 interactions and for virus stability.

Rotaviruses are the major viral pathogens that cause severe gastroenteritis in young children and animals throughout the world (13, 19). The significance of rotavirus infections has stimulated research efforts to develop effective methods of disease prevention and control (7, 19).

The rotavirus outer capsid proteins VP4 and VP7 are involved in neutralization of rotavirus infectivity and are capable of inducing a protective immune response in some experimental animal models (7, 25, 26, 31, 32). Neutralization of rotavirus infectivity by antibodies has been proposed as one mechanism of immunological defense against rotavirus infection (10, 17, 25, 30). However, the antigenic structure of rotavirus is complex, and individual epitopes can be affected by glycosylation and interactions of specific combinations of the outer capsid proteins (4, 5). Therefore, understanding the structure, interactions, and functions of the rotavirus outer capsid proteins is important for both theoretical and practical reasons.

Monoclonal antibodies (MAbs) to rotavirus VP4 and VP7 can neutralize rotavirus infectivity in vitro and in vivo (24–26, 38–40). We initially characterized six epitopes on VP4 of simian rotavirus SA11 clone 3 (Cl3) by using 13 MAbs (3). Three neutralization-positive epitopes (NP1 to NP3) and three neutralization-negative epitopes (NN1 to NN3) were identified. NP1 was further subdivided into sites NP1a and NP1b on the basis of differences in biological properties and competitive MAb capture enzyme-linked immunosorbent assay (ELISA) reactivities. NP1b MAbs showed reciprocal competition with each other. However, when NP1a MAbs were used as capture MAbs and the NP1b 7G6 MAb was used as the competition MAb, only a one-way competition was seen. Partial competition was detected between NP1a MAbs and the NP1b MAb 10G6 when the 10G6 MAb was used as the capture MAb.

The NP1 epitope appeared to be unique, because a positive cooperative binding was observed when any of the NP1 MAbs were used as the competing MAb with any of the nonneutralizing MAbs as the capture MAb. These data indicated that a conformational change might occur with the binding of NP1 MAbs to the rotavirus VP4 and that the mechanism for rotavirus neutralization by the NP1 MAbs might be a novel one.

This paper reports studies which examined the effect of NP1 to NP3 MAbs on the structure and function of SA11 VP4. We examined the direct effect of NP1b MAb binding on virus structure and characterized four neutralization escape mutants selected with the neutralization MAbs 9F6, 7G6, 10G6, and 23.

MATERIALS AND METHODS

Cells, viruses, rNV particles, and MAbs. MA 104 cells were grown in medium M199 containing 5% fetal calf serum. Our

* Corresponding author. Phone: (713) 798-3585. Fax: (713) 798-3586.

† Present address: Department of Medicine, Stanford University, Palo Alto, CA 94304.

‡ Present address: Department of Pediatrics, Hakodate Municipal Hospital, Yayoicho 2-33, Hakodate, Hokkaido 040, Japan.

§ Present address: Department of Laboratory Medicine, Kinan General Hospital, 510 Minato, Tanabe City 646, Wakayama, Japan.

standard laboratory virus, SA11 Cl3, was used as the parental virus and was prepared, radiolabeled with Tran^{35}S, and purified as previously described (11, 12).

Radiolabeled recombinant Norwalk virus (rNV) particles were expressed and purified from insect cells infected with a baculovirus recombinant as previously described (18). Briefly, 36 h postinfection, the medium was replaced with an equal volume of Grace's medium which contained 10 μCi of a ^{3}H-labeled L-amino acid mixture (1 mCi/ml [ICN, Irvine, Calif.]) per ml and incubated at 29°C for 4 days. The supernatant was collected and clarified by centrifugation for 10 min at 8,000 rpm in a Beckman JA-14 rotor and then concentrated by pelleting through a 45% sucrose cushion in 0.1 M phosphate-buffered saline (PBS [pH 7.4]) for 2 h at 26,000 rpm in a Beckman SW 28 rotor. The pellets were suspended in CsCl-PBS (1.362 g/ml) and centrifuged for 18 h at 35,000 rpm in a Beckman SW 50.1 rotor. The band containing rNV particles was collected by side puncture, and the rNV particles were diluted and pelleted by centrifugation for 2 h at 35,000 rpm in a Beckman SW 40.1 rotor to remove the CsCl. The purified radiolabeled rNV particles were used as an internal control for the sucrose density gradients.

The MAbs to SA11 Cl3 VP4, 3C8 (NN1), 9F6 (NP1a), 10G6, and 7G6 (NP1b) were generated and characterized previously by our laboratory (3). A MAb to porcine rotavirus (OSU) VP4, 2G4 (NP2), and MAbs to rhesus rotavirus (RRV) VP4, 23 (NP3), and RRV VP7 MAb 60 (nonneutralizing) were obtained from Harry Greenberg (Stanford University, Palo Alto, Calif.). MAbs purified by high-pressure liquid chromatography were used in immune electron microscopic (IEM) analysis, ELISA, and hemagglutination (HA) and hemagglutination inhibition (HI) assays, and ascitic fluids were used for selecting neutralization escape mutants and for plaque reduction neutralization assays (PRNAs).

IEM analysis of SA11-MAb complexes. SA11 (cesium chloride-purified triple-layered particles) was activated by trypsin and diluted in 1% bovine serum albumin (BSA)–PBS to a concentration of 30 μg/ml. A 200-μl aliquot of diluted SA11 was mixed with 200 μl of each of the MAbs (10 μg in PBS) 9F6, 7G6, 10G6, 23, and 2G4 or PBS and incubated 1 h at 37°C. A 40-μl aliquot of each virus-antibody mixture was added to carbon-coated 400-mesh copper grids with 2% Parlodion support film and stained with 1% ammonium molybdate (pH 5.5). A 20-μl aliquot of each virus-antibody mixture was used for PRNA, and a 340-μl aliquot of each virus-antibody mixture was analyzed by sucrose gradient centrifugation.

Sucrose gradient analysis of SA11-MAb complexes. A 340-μl aliquot of each virus-antibody complex was added to the top of a 15 to 45% continuous sucrose density gradient (10 ml) on a 60% CsCl cushion (1 ml). As an internal control, a 10-μl aliquot of ^{3}H-labeled rNV particles also was added to each gradient before centrifugation. The gradients were centrifuged for 40 min with a Beckman SW 40.1 rotor at 35,000 rpm at 4°C, and 0.3-ml fractions were collected. The radioactivity in each fraction was determined by using a double-labeling program and counting 50 μl from each fraction in a Beckman scintillation spectrometer (LS 3801). A 40-μl aliquot of each fraction was mixed with 2× electrophoresis sample buffer, boiled, and examined by sodium dodecyl sulfate-polyacrylamide gel electrophoresis (SDS-PAGE) (10% polyacrylamide) as described previously (3).

Selection and characterization of neutralization escape mutants by plaque assay and PRNA. SA11 VP4 neutralization escape mutants were selected with the four neutralization MAbs 9F6, 10G6, 7G6, and 23. SA11 (10^7 PFU/ml) was preactivated with 10 μg of trypsin per ml and diluted to 10^{-2} to 10^{-3} with PBS. MAb ascitic fluid was prepared by dilution to 1:500, 1:1,000, and 1:2,000 for MAbs 10G6, 7G6, and 9F6 and dilution to 1:200, 1:400, and 1:800 for MAb 23. Equal volumes of diluted virus and selecting MAb were combined and incubated for 1 h at 37°C. Each virus-MAb mixture (200 μl) was inoculated onto MA104 cell monolayers and incubated for 1 h at 37°C. After washing the cells three times to remove the residual inoculum, medium M199 lacking fetal calf serum but containing each diluted MAb and 2 μg of trypsin per ml was added, and the cells were incubated at 37°C. When the cytopathic effect was observed, the virus was harvested and titrated by plaque assay. This procedure was performed at least twice for each MAb tested. Putative mutants from the highest dilution of virus and the lowest dilution of MAb were chosen to undergo a second round of selection. The virus isolated from the last selection was plaque purified three times and characterized by PRNA as previously described (11, 12). Isolated plaques were grown in the presence of the selecting MAb. Two isolates for each escape mutant were selected independently. Each escape mutant resistant to neutralization by the selecting MAb is indicated by an "R."

Two types of PRNAs were performed in this study. The first type of PRNA was performed to characterize the escape mutants. Approximately 40 to 50 PFU of virus per well was incubated with serial dilutions of each MAb tested, and then each virus-MAb mixture was plaqued. Serial 10-fold dilutions of each MAb were made starting at 1:100. The final dilutions tested were 800,000 for MAb 10G6, 80,000 for MAb 7G6, 8,000 for MAb 9F6, and 800 for MAb 23. These end points were tested on the basis of the neutralization titers of each MAb with the parental virus (3). This type of neutralization analysis determined whether each test MAb neutralized parental and mutant virus infectivity. In addition, we used this test format to determine the neutralization titer of each MAb (a >60% reduction of virus plaques was considered significant). The second type of PRNA was performed to determine the total neutralization activity of each MAb with the parental SA11 virus. In this assay, virus (approximately 10^8 PFU/ml) was incubated with serial dilutions of each test MAb. After the virus was incubated with the MAb, the virus-MAb mixture was diluted and plaqued. By comparison of the total virus titer (PFU per milliliter) obtained after incubation with PBS and the titer obtained after incubation with each MAb concentration, we determined the total amount (log decrease) of neutralization of virus infectivity.

Antigen capture ELISA, HA, and HI assays. MAb binding to virus was assessed by ELISA as previously described with an antigen capture technique (3). Briefly, 96-well plates were coated with each purified MAb (2 μg/ml) diluted in PBS and incubated overnight at 4°C. The plates then were blocked for 2 h at 37°C with 3% BSA–PBS. Purified escape mutants and SA11 were diluted to concentrations of 1, 2, 4, and 8 μg/ml with PBS. After the plates were washed, each virus dilution was added, and the plates were incubated for 1 h at 37°C, which was then followed by the addition of detector guinea pig serum (no. 504, a hyperimmune guinea pig serum made to purified SA11 triple-layered particles), horseradish peroxidase-conjugated goat anti-guinea pig immunoglobulin G antibody (Hyclone Laboratory, Logan, Utah), and substrate 2,2′-azinobis-3-ethylbenzthiazoline sulfonic acid (Sigma Chemical Co., St. Louis, Mo.), respectively. The optical density at 414 nm (OD_{414}) of the wells was determined after a 30-min incubation at 37°C.

Human type O erythrocytes were used to test purified virus HA and HI activity of MAbs in 96-well microtiter plates as previously described (3). HI assays were performed by using

serial twofold dilutions of purified MAb (starting at 20 μg/ml), and 4 HA units of purified virus were used per test well.

One-step growth curves of neutralization escape mutants and parental virus. Confluent MA 104 monolayers in 25-cm^2 flasks were infected with 9F6R, 10G6R, 7G6R, 23R, and SA11, respectively, with a multiplicity of infection of 5 PFU/ml. At 2, 4, 6, 8, 10, 12, 14, 18, 24, 36, 48, 72, and 96 h postinfection, two flasks for each virus were harvested. Virus yield at each time point was determined by plaque assay as previously described (12).

Sequencing of neutralization escape mutants and parental virus. To sequence gene 4, cDNA was synthesized by reverse transcription (reverse transcriptase from avian myeloblastosis virus [Life Science Inc., St. Petersburg, Fla.]), and PCR (*Taq* DNA polymerase from Perkin-Elmer Co., Norwalk, Conn.) from either double-stranded RNA or mRNA of the escape mutants and parental virus with SA11 gene 4-specific primers (5′-end primer, 3′-end primer, and internal primers) as described previously (1). The PCR products were resolved in 1% low-melting-point agarose (SeaPlaque [FMC BioProducts, Rockland, Maine]) with 0.04 M Tris-acetate and 0.001 M EDTA running buffer. The specific DNA bands were eluted and sequenced directly by Sanger's method with a DNA sequencing kit (Sequenase, version 2.0 [U.S. Biochemical Corp., Cleveland, Ohio]). Each mutation site was confirmed by sequencing two independent reverse transcription-PCR products.

To obtain the gene 9 sequence of 10G6R and SA11, the cDNAs were synthesized by reverse transcription-PCR with gene 9 primers (5′- and 3′-terminal primers) and cloned into the pCR 1000 vector (TA Cloning System [Invitrogen Co., San Diego, Calif.]). Recombinants containing gene 9 inserts were then sequenced with the DNA sequencing kit.

RESULTS

IEM and sucrose gradient analysis of SA11-MAb complexes. The NP1 MAbs were of interest because our previous ELISA data had suggested that conformational changes occur following SA11 binding to NP1 MAbs. We sought to directly determine if NP1 MAbs induced conformational changes in virus structure as one mechanism of virus neutralization. To test this hypothesis, virus-MAb complexes were prepared and aliquots were analyzed by electron microscopy (EM [Fig. 1]), sucrose gradient centrifugation and SDS-PAGE (Fig. 2), and PRNA. EM analysis showed that virus incubated with PBS was well dispersed (Fig. 1A). In contrast, SA11 triple-layered particles were disassembled with the binding of NP1b MAbs 10G6 and 7G6 (Fig. 1B and C). The virus outer capsid was partially or completely removed. Broken virus particle debris was observed, and PRNA showed that total virus infectivity was reduced 3 and 5 logs for MAbs 7G6 and 10G6, respectively. When SA11 was incubated with the NP1a MAb 9F6, NP2 MAb 2G4, and NP3 MAb 23, significantly more virus aggregates were observed than in the PBS-virus control (Fig. 1A, D, E, and F). These virus-MAb particles remained intact, although PRNA showed total virus infectivity was reduced 4 logs, 3 logs, and 1 log, respectively. The NP2 MAb 2G4, which binds on the sides near the tip of the dimeric spike (33), was used as a control for these experiments. Virus with MAb 2G4 immunoglobulin G complexes was clearly visible (Fig. 1E).

The sucrose gradient profiles of radiolabeled control virus showed that the peak of an internal control, ^{3}H-labeled rNV particles, was in fractions 5 to 7 (Fig. 2), the peak of ^{35}S-labeled triple-layered rotavirus particles was in fractions 23 and 24 (Fig. 2A, double shelled [ds]) and the peak of ^{35}S-labeled double-layered rotavirus particles was in fractions 20 and 21 (Fig. 2C, single shelled [ss]). When virus-NP1b MAb 10G6 complexes were analyzed, the peak for triple-layered particles (ds) was not seen, but the peak in the position for double-layered particles (ss, fractions 19 to 21) was increased significantly, and a large amount of radioactivity (^{35}S-labeled proteins) was observed as soluble proteins in the top two fractions of the gradient (Fig. 2B). Similar results were seen with virus-NP1b MAb 7G6 complexes (data not shown). When the NP1a MAb 9F6-, NP2 MAb 2G4-, and NP3 MAb 23-virus complexes were analyzed (Fig. 2D to F), the peak of triple-layered particles (ds) was decreased significantly compared with that of the virus-PBS control (Fig. 2A), and more radioactivity (^{35}S-labeled proteins) was observed in the fractions at the bottom of the centrifuge tubes (Fig. 2D to F).

To confirm that the shift in the peak of radioactivity from fractions 23 and 24 (the ds peak) to fractions 19 to 21 (the ss peak) observed with the virus-NP1b MAb 10G6 complexes represented the removal of the outer capsid proteins (Fig. 2B), we analyzed the peak fractions by SDS-PAGE to determine their protein compositions. SDS-PAGE data showed that the outer capsid proteins were observed in the top two fractions and not in fractions 18 to 24 when the NP1b MAbs were mixed with virus (Fig. 2B, the upper panel). Released soluble proteins were not observed in the top fractions of gradients after virus was incubated with PBS (Fig. 2A, the upper panel) or with the NP1a, NP2, or NP3 MAbs (data not shown). However, all of the virus capsid proteins VP2, VP6, VP4, and VP7 were observed in the fractions at the bottom of the centrifuge tube (fractions 25 to 39) when NP1a, NP2, and NP3 MAb-virus complexes were analyzed (data not shown). The appearance of all of the capsid proteins in these faster-migrating fractions indicated they represented virus-MAb aggregates whose migration shifted to the bottom fractions of the gradients.

Selection and characterization of neutralization escape mutants. To localize the neutralization site involved in antibody-induced conformational changes on SA11, we selected four neutralization escape mutants designated 9F6R, 10G6R, 7G6R, and 23R, with NP1a MAb 9F6, NP1b MAbs 10G6 and 7G6, and NP3 MAb 23, respectively. PRNAs were performed to confirm that each mutant virus escaped neutralization by the selecting MAb (Fig. 3). The neutralization escape mutant 9F6R was not neutralized by the homologous NP1a MAb 9F6 but was neutralized by heterologous NP1b MAbs 10G6 and 7G6 and NP3 MAb 23 (Fig. 3A). Similar results were obtained for the NP1b neutralization escape mutants 10G6R and 7G6R and the NP3 mutant 23R (Fig. 3B, C, and D).

Properties of the neutralization escape mutants. We next compared the binding and other biological properties of the neutralization escape mutants with those of the parental SA11 virus.

(i) Binding activity of neutralization escape mutants to the selecting MAbs. To examine whether the escape mutants still could bind the selecting MAb, the mutants and parental virus were tested with an antigen capture ELISA (Fig. 4). Two nonneutralizing MAbs, NN1 MAb 3C8 to SA11 VP4 and MAb 60 to RRV VP7, were used as controls to monitor the amount of virus used in each assay. With increasing concentrations of virus, SA11 binding to each MAb increased, but no binding of any of the escape mutants with their respective selecting MAbs or homologous MAbs was observed. The binding of the parental SA11 virus to the selecting MAbs was greater than the binding of the escape mutants to these MAbs (Fig. 4A, B, and C), except in the case of the NP3 MAb 23 (Fig. 4D). The binding activities of the NP1b escape mutants (7G6R and 10G6R) to NP1a MAb 9F6 were similar (Fig. 4A), but the

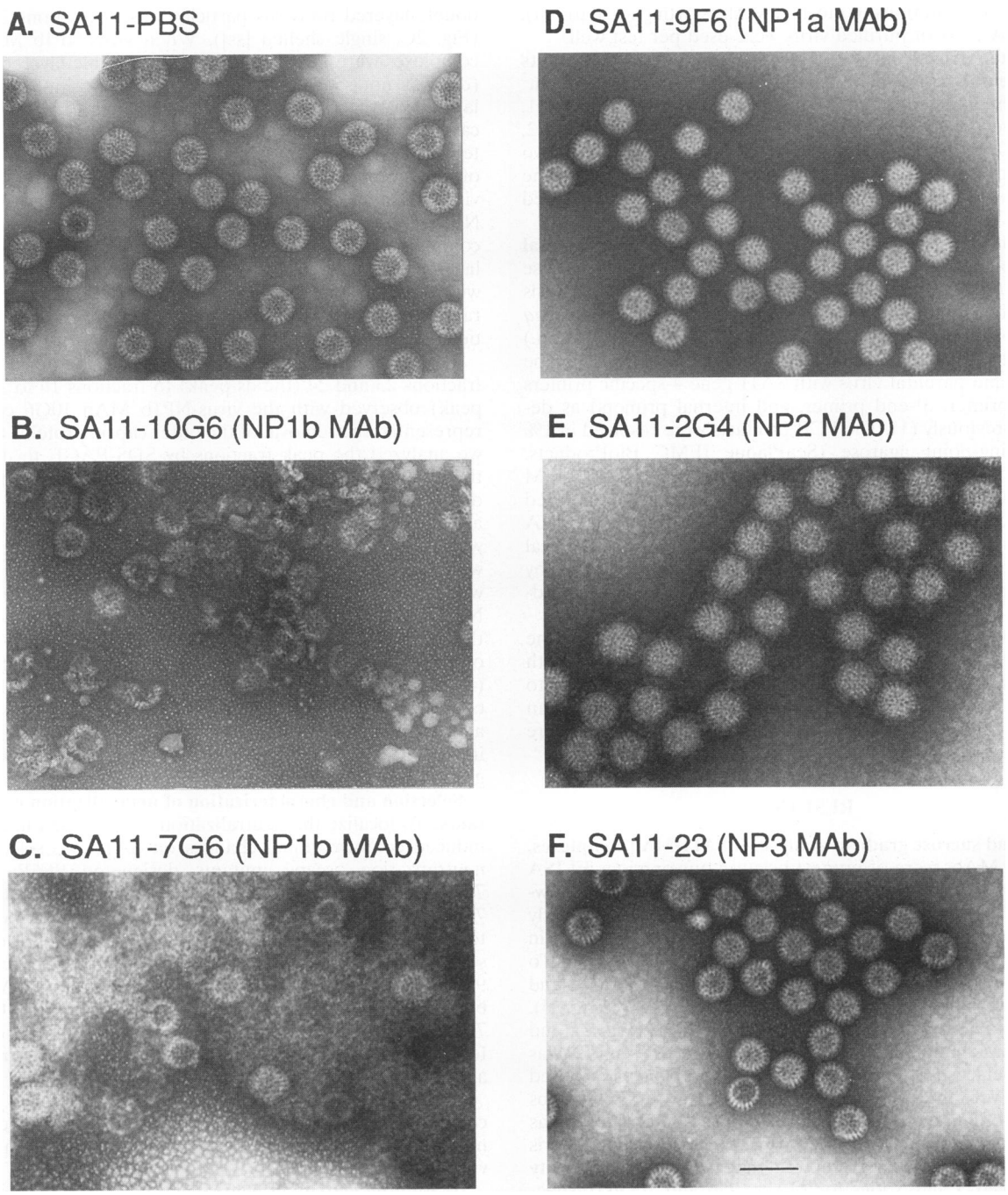

FIG. 1. IEM analysis of SA11-MAb complexes. SA11 triple-layered particles (200 μl of 30-μg/ml virus) were incubated with PBS (A) (200 μl), MAb 10G6 (B) (10 μg/200 μl), MAb 7G6 (C) (10 μg/200 μl), MAb 9F6 (D) (10 μg/200 μl), MAb 2G4 (E) (10 μg/200 μl), or MAb 23 (F) (10 μg/200 μl) for 1 h at 37°C. The complexes, put onto EM grids, were stained with 1% ammonium molybdate. The immunoglobulin G complexes of MAb 2G4 clearly bind on the sides near the end of the dimeric spikes (33). Bar, 100 nm.

binding activity of the NP1a escape mutant 9F6R to the NP1b MAb 7G6 was distinguishable and poor relative to the binding of 9F6R to the NP1b MAb 10G6 (Fig. 4B and C). The NP3 mutant 23R showed good binding to the NP1b 7G6 MAb, and the reciprocal binding of the NP1b 7G6R escape mutant to NP3 MAb 23 was also strong (Fig. 4C and D). This latter result was of interest, because MAb 23, which originally was made to RRV, bound poorly to the parental SA11 virus (Fig. 4D).

Unexpected results were observed with the control reactions. The binding of all of the escape mutants to VP4 MAb 3C8 was similar to the binding activity of the parental SA11 virus (Fig. 4E; $P > 0.05$), but the binding of all of the NP1 MAb escape mutants (10G6R, 7G6R, and 9F6R) to VP7 nonneutralizing MAb 60 was stronger than the binding activity of the parental SA11 virus (Fig. 4F; $P < 0.001$). Because the ELISA binding activity of the NP1 escape mutants to nonneutralizing

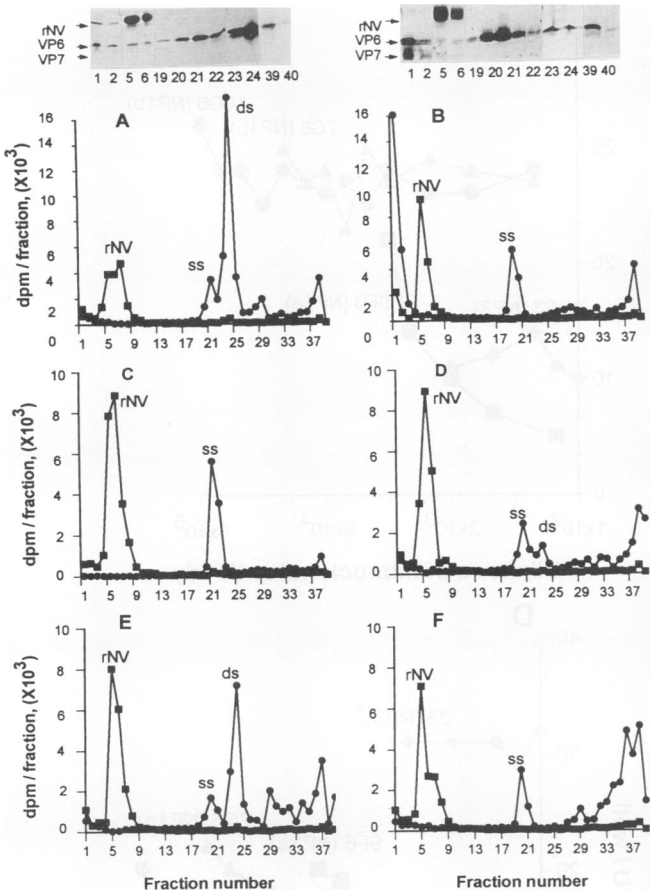

FIG. 2. Analysis of SA11-MAb complexes by the sucrose density gradients (A to F) and SDS-PAGE (above panels A and B). Tran^{35}S-labeled SA11 (●) ds particles (200 μl of 30-μg/ml virus) incubated with PBS (A) (200 μl), MAb 10G6 (B) (10 μg/200 μl), MAb 9F6 (D) (10 μg/200 μl), MAb 2G4 (E) (10 μg/200 μl), and MAb 23 (F) (10 μg/200 μl) for 1 h at 37°C. (C) Tran^{35}S-labeled SA11 ss particles (200 μl of 30-μg/ml virus) were incubated with PBS for 1 h at 37°C. A 10-μl aliquot of ^{3}H-labeled rNV particles (■) was added to each gradient before centrifugation as an internal control. The ds and ss represent the peaks containing the triple-layered and double-layered virus particles, respectively. Fraction 1 of the sucrose density gradient profiles represents the top of the gradients.

MAb 60 was increased (Fig. 4F), PRNA was performed to determine if an alteration of the NP1 epitope might have mediated a change in the neutralization properties of the MAb 60 epitope. The 10G6R mutant was examined. This mutant behaved like the parental SA11 virus; no neutralization of the 10G6R mutant by MAb 60 was observed (data not shown).

(ii) HA and HI activity of neutralization escape mutants. Biological studies of purified preparations of the escape mutants and the SA11 virus found that the mutants 10G6R, 7G6R, and 9F6R (10 μg/ml) possessed HA activity with human type O erythrocytes, but 23R (100 μg/ml) lacked HA activity. In addition, no HI activity with the selecting MAbs was observed with the escape mutants 10G6R, 7G6R, and 9F6R, although HI activity was observed with the parental SA11 virus. With the parental SA11 virus, HI activity was seen with as little as 0.156 μg of 10G6 MAb per ml, while the 10G6R mutant still showed HA activity, even in the presence of 20 μg of MAb 10G6 per ml.

(iii) Plaque phenotype of neutralization escape mutants. The mutants 10G6R and 23R produced significantly larger plaques (1 to 3 mm) than the parental SA11 virus (0.5 to 1.5 mm) on the first day of the second overlay. Also, the plaques appeared earlier than did the plaques of the parental SA11 virus. The plaques of these mutants appeared on the first day following the second overlay, while the SA11 plaques mainly appeared on the second day after the second overlay. These biological properties were similar to those of the variant SA11 4F virus (4 to 6 mm [2]). However, in contrast to the different properties of SA11 4F and SA11 Cl3, none of the neutralization escape mutants produced any plaques when trypsin or pancreatin was omitted from the overlay. In addition, no significant differences in the protein profiles by Western blot (immunoblot) or in the RNA profiles were found between the mutants and the SA11 virus (data not shown). These results indicate that the properties of gene 4 of these mutants are different from those for SA11 4F.

(iv) One-step growth curves of neutralization escape mutants. To determine if the mutants had unusual growth properties, one-step growth curves of the escape mutants and parental SA11 virus were compared (Fig. 5). Parental virus SA11 and the NP1 escape mutants 9F6R, 10G6R, and 7G6R had similar growth curves, showing similar peak titers and growth kinetics. The NP3 escape mutant 23R had similar growth kinetics, but the maximal titer obtained was lower than that for SA11. Also, the infectivity of 23R appeared to be less stable after 8 h postinfection.

Nucleotide sequence of gene 4 of neutralization escape mutants. Sequence analyses were performed for gene 4 of the four neutralization escape mutants and the parental SA11 virus to determine the nucleotide substitutions (Table 1). For the mutant 10G6R, sequence analysis of gene 4 found a one-nucleotide change from A to G in position 556, which would result in an Asn-to-Asp change in aa 183 of VP4. The sequences of gene 9 of 10G6R and SA11 were identical. One amino acid change also was observed on VP4 at aa 136 for 9F6R, aa 180 for 7G6R, and aa 194 for 23R, respectively. All of the mutated sites mapped to VP8* of VP4 within the HA domain (14, 20). The same amino acid substitutions were found when the sequences of one other mutant selected independently for each MAb were compared. To determine whether the amino acid substitutions observed in the NP1b-resistant viruses were unusual, we compared the amino acid sequences around the NP1b epitope with the VP4 sequences reported for all of the group A rotaviruses. The comparisons showed that the amino acid substitutions in the mutants that resulted in a charged residue at aa 180 or 183 were not seen in other strains; in addition, aa 180 and 183 flank a proline residue (aa 182) which is conserved in all of the group A rotaviruses except bovine rotavirus B223 (Fig. 6).

DISCUSSION

In these studies, we directly determined the effect of NP1-NP3 MAbs on the structure and function of SA11 VP4 by EM, sucrose density gradient centrifugation, and PRNA analysis. We found that triple-layered particles disassembled as a result of binding to NP1b MAbs 7G6 and 10G6 but not as a result of binding to NP1a MAb 9F6, NP2 MAb 2G4 (amino acid substitution of MAb 2G4 escape mutant at aa 393), and NP3 MAb 23. SA11 infectivity was reduced 3 and 5 logs by MAbs 7G6 and 10G6, respectively. These results suggest that the NP1b MAbs bind to a critical site for virus stability, and the mechanism for rotavirus neutralization by the NP1b MAbs might be a novel one. Antibody-induced conformational

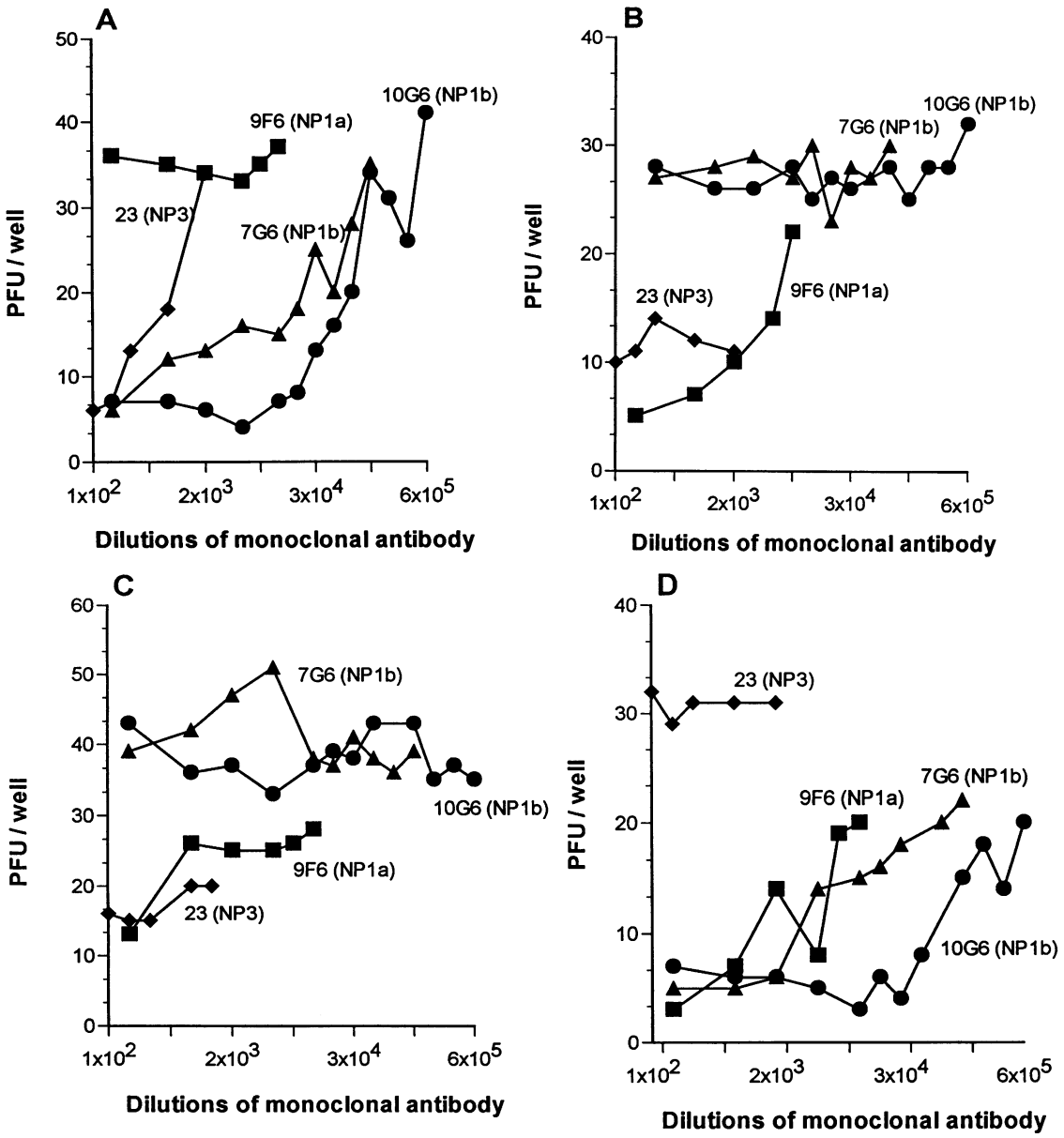

FIG. 3. Characterization of neutralization escape mutants with homologous and heterologous MAbs by PRNA. The panels show testing of the following neutralization escape mutants in six-well plates: 9F6R (A) (39 ± 1 PFU per well), 10G6R (B) (29 ± 2 PFU per well), 7G6R (C) (40 ± 4 PFU per well), and 23R (D) (34 ± 1 PFU per well). The neutralization titers of each MAb with parental virus SA11 were 400,000 for MAb 10G6, 40,000 for MAb 7G6, 4,000 for MAb 9F6, and 400 for MAb 23.

changes have been reported as one mechanism of virus neutralization in poliovirus, foot-and-mouth disease virus, influenza virus, and adenovirus (8, 9, 22, 29, 41). Electron cryomicroscopy and image processing have shown that 60 dimeric VP4 spikes are positioned at the edge of type II channels, and these VP4 spikes interact with VP7 and VP6 (33, 34, 36). An alteration of VP4 structure upon binding of VP4 to NP1b MAbs may change the interactions between VP4 and VP7. Such conformational changes in virus structure could be detrimental to infectivity and could be the basis of neutralization by the NP1b MAbs. The EM analyses also were striking because the results showed that virus spikes decorated with MAb 2G4 are clearly visible, but the binding of the other VP4 MAbs to different regions of the spikes cannot be seen clearly. These results suggest that the location of MAb binding on the spike influences how clearly the MAb can be seen. Thus, MAb 2G4, which binds to the distal region of VP4 spikes (33), is easily seen, while the other MAbs, which bind to the VP8* domain of VP4, are not seen clearly. Because our other data with these MAbs suggest that the VP8* domain is located closer to the base of the spikes near VP7, we hypothesize that the VP8* domain of VP4 is the one that interacts with VP7 and VP6.

We localized the neutralization sites for NP1 and NP3 by selecting and characterizing the four neutralization escape mutants 9F6R, 7G6R, 10G6R, and 23R by using the MAbs

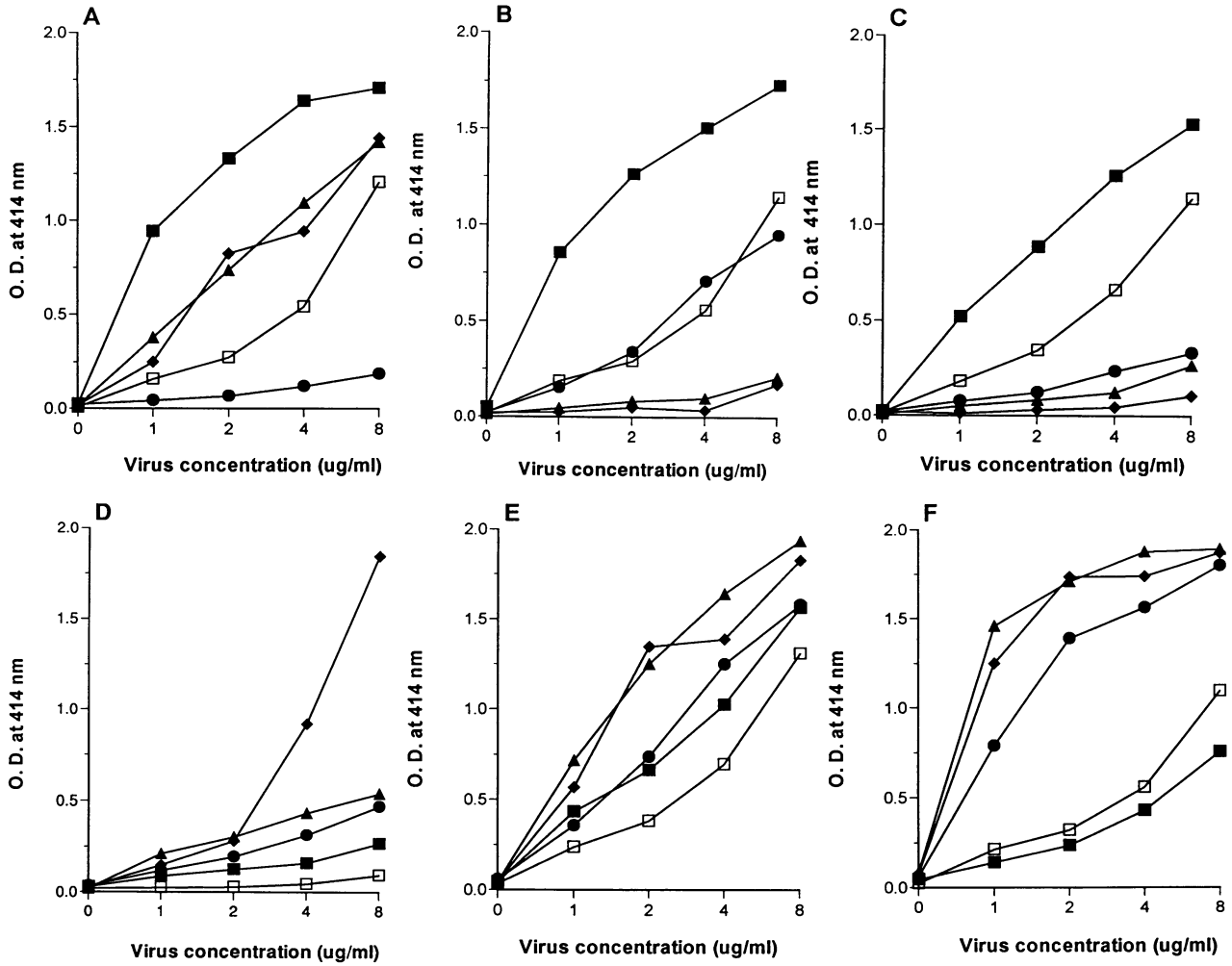

FIG. 4. Binding activity of neutralization escape mutants and parental virus SA11 to VP4 MAbs. (A) 9F6, an NP1a MAb to VP4 of SA11; (B) 10G6, an NP1b MAb to VP4 of SA11; (C) 7G6, an NP1b MAb to VP4 of SA11; (D) 23, an NP3 MAb to VP4 of RRV; (E) 3C8, an NN1 MAb to VP4 of SA11; (F) 60, a nonneutralizing MAb to VP7 of RRV. An antigen capture ELISA was used to test and compare the ability of escape mutants and SA11 to bind each MAb. Ninety-six-well plates were coated with each purified MAb. One hundred microliters of 1-, 2-, 4-, and 8-μg/ml cesium chloride-purified triple-layered virus particles was then added, followed by the addition of detector serum (guinea pig anti-SA11), horseradish peroxidase-conjugated immunoglobulin G and substrate (2,2′-azinobis-3-ethylbenzthiazoline), respectively. The OD_{414} was determined after a 30-min incubation. ■, SA11; ▲, 10G6R; ◆, 7G6R; □, 23R; ●, 9F6R.

9F6, 7G6, 10G6, and 23, respectively. Characterization of the properties and determination of the amino acid substitutions in these mutants confirmed they are truly escape mutants and supported the previous assignments of the NP1a, NP1b, NP2, and NP3 MAbs into separate epitopes. Compared with the parental virus SA11, the escape mutants did not bind to the selecting MAbs by ELISA. These results suggested that the mutants escaped neutralization by not binding to the selecting MAbs because of the changes in amino acid sequence or an alteration in the conformation of the epitopes on the mutants.

The hypothesis that the epitopes were altered was further supported by the ELISA reactivity of the NP1b mutants 10G6R and 7G6R with the nonneutralizing MAb to VP7. Binding of 10G6R and 7G6R to VP7 MAb 60 was stronger than the binding of these MAbs to the parental SA11 virus. One explanation for these results is that an alteration of the NP1 epitope of VP4 caused changes in other epitopes on VP7 and affected the interactions between these two outer capsid proteins. This is consistent with the hypothesis that the NP1b MAbs affect virus stability, VP4-VP7 interactions, or both. Reassortant analysis of rotavirus also showed that the interaction of VP4 with different VP7s affects expression of the VP4-specific epitope 2G4 (5). The stronger binding of the VP8* NP1b mutants with the nonneutralizing MAb 60 was interesting because MAb 60 has been mapped to VP7. We investigated whether alteration of an NP1b epitope could result in a change in the nonneutralizing property of MAb 60. Like the parental SA11 virus, 10G6R was not neutralized by MAb 60. These results indicated that the increased ELISA reactivity after binding to MAb 60 was not due to particle instability. In addition, the MAb 60 epitope is not an essential site for virus infectivity. We concluded that the alteration of the NP1b epitope enhances the exposure of the MAb 60 epitope and permits these epitopes on the NP1b mutants to strongly bind MAb 60. An alternative explanation is that the mutations alleviate steric hindrance from VP8* that prevents antibody access to VP7.

The neutralization mechanisms for MAbs 9F6 and 23 are

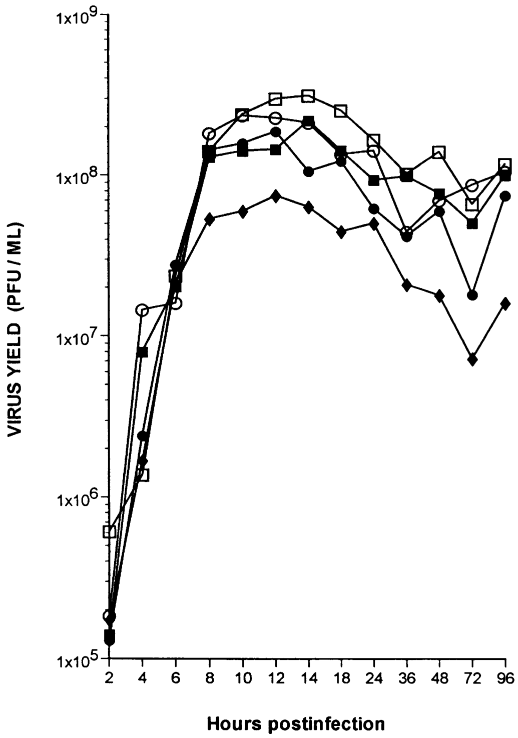

FIG. 5. Comparative one-step growth curves for neutralization escape mutants 9F6R (NP1a [□]), 7G6R (NP1b [■]), 10G6R (NP1b [●]), and 23R (NP3 [◆]) and parental virus SA11 Cl3 (○). At each time point, virus yield was determined by plaque assay. Mean growth curves were generated for total infectious yield (n = 4).

```
             172           ↓     ↓                    200
SA11      GKIYTYNG ET [P] NANTGYY STTN.FDTVN
SA11-4F   GKIYTYNG ET [P] NANTGYY STTN.FDTVN
RRV       GKIYTYNG ET [P] NVTTKYY STTN.YDSVN
SA11-SEM  EKLYTYEG QT [P] NARTGHY STTN.YDSVN
69M       GQLWTYNG ET [P] NAITNGY PTTN.YDSVN
OSU       GRIYTYNG TT [P] NATTGYY SATN.YDTVN
H-2       GQLWVYNG ET [P] NATTTGY VTSN.YDSLT
UK        RRLFIYEG ET [P] NATTKGY FITN.YASAE
K8        NRVYWYQG AT [P] NASESYY LTIN.NDNSN
DS1       GRVWTFHG ET [P] RATTDSS NTAD.LNNIS
Wa        GRVWTFHG ET [P] RATTDSS STAN.LNNIS
GOTT      GRVWTFNG ET [P] HATTDYS TTSN.LPDVE
M37       NSVWTFHG ET [P] HATTDYS STSN.LSEVE
B223      GNISNYWG AD  T  QGDLRVG TYSNPVPNAV
```

FIG. 6. Comparison of VP4 sequences of group A rotaviruses surrounding the NP1b region. The arrows show the positions of amino acid substitutions seen in the sequences of the NP1b neutralization escape mutants, and the conserved proline residue is boxed. The accession numbers for the sequences shown (from top to bottom) are P04508, X57319, P12473, P17464, P26451, P11114, L04638, P12474, D90260, P11196, P11193, P23045, P11197, and M92986. The data bank source of the sequence accession numbers is denoted by the first letter of the accession number, as follows: P, SWISS-prot; X, D, L, M, GenBank.

still unclear, but our data suggest that NP1a MAb 9F6 and NP3 MAb 23 can inhibit parental virus binding to cells when total virus infectivity is neutralized 4 logs and 1 log, respectively (unpublished data). Binding of the NP1a mutant 9F6R to VP7 MAb 60 was stronger than the binding of this MAb to the parental SA11 virus, but EM and sucrose gradient analyses revealed that virus aggregates occurred and that viruses remained intact when MAb 9F6 bound to the parental virus. It remains unknown whether MAb 9F6 binding to virus results in an alteration of VP4 conformation only or blocking of VP4 binding to cells to mediate neutralization of virus infectivity.

Biological studies of the escape mutants found that all of the NP1 escape mutants could hemagglutinate human type O erythrocytes. However, these mutants completely escaped HI with the selecting MAbs. These results indicate that the NP1 neutralization epitopes must be located in the HA domain, but they apparently are not critical for HA activity. The alteration of epitopes within the HA domain results in loss of binding of 9F6R, 7G6R, and 10G6R with the MAbs 9F6, 7G6, and 10G6, respectively, which would explain the lack of HI activity. Of particular interest, the NP3 MAb escape mutant 23R lacked HA activity and produced lower peak titers in one-step growth curves. These results suggest that the MAb 23 epitope may be critical for HA function.

TABLE 1. Nucleotide and amino acid changes on gene 4 of escape mutants

Escape mutant	Epitope	Protein specificity	Change	
			Nucleotide (bp)	Amino acid (location)
9F6R	NP1a	VP4 (VP8*)	G→A (415)	Asp→Asn (136)
7G6R	NP1b	VP4 (VP8*)	A→G (548)	Gln→Arg (180)
10G6R	NP1b	VP4 (VP8*)	A→G (556)	Asn→Asp (183)
23R	NP3	VP4 (VP8*)	A→G (590)	Tyr→Cys (194)

Like SA11 4F, mutants 10G6R and 23R produced larger plaques than parental SA11 Cl3; in contrast to SA11 4F, 10G6R and 23R did not produce plaques without trypsin or pancreatin in the overlay (2). SA11 4F differs from SA11 Cl3 at 131 aa residues, including the neutralization epitopes at aa 88, 89, 100, 114, 148, and 188 in VP8* and aa 388, 393, and 440 in VP5* (28). The 10G6R mutant showed a one-step growth curve similar to that of SA11, while 23R produced lower peak titers in a one-step growth curve. It is unclear if the larger plaque phenotype is related to the sequences around aa 183 and 194 in VP8*. However, SA11 4F cannot be neutralized by NP1 MAbs (3); the lack of reactivity with the NP1 MAbs might be explained by the sequence differences at aa 148 and 188 in SA11 4F.

Sequence analyses of gene 4 of these mutants found 1 aa substitution in VP8* for each mutant. These amino acid substitution sites are located within the HA domain mapped between aa 47 and aa 247 (14, 20). It is interesting to compare these three NP antigenic sites on SA11 with those reported on VP4 by others (23, 37, 39, 40). Our NP1 site is unique and divided into two subepitopes as suggested by our earlier competition experiments (3), and no previous MAbs to VP4 have been mapped to the same sites. The NP1a 9F6 amino acid substitution is located in residue 136. This residue is altered from a highly charged amino acid to a neutral amino acid (Asp to Asn). The NP1b epitope 7G6 is included in one of the sites mapped by characterization of SA11 4fm selected with hyperimmune serum (15). NP1b epitopes 7G6 (Gln to Arg) and 10G6 (Asn to Asp) are altered from neutral amino acid to highly charged amino acid, which might result in conformational changes in VP4 structure. The amino acid substitutions in the NP1b escape mutants (aa 180 and aa 183) flank a proline residue that is conserved in all VP4s of group A rotaviruses published except bovine rotavirus B223 (16, 21, 27). This is of interest because the outer capsid of B223 exhibits little stability

during standard rotavirus purification procedures, and the property of instability segregates with gene 4 (6). It is possible that lack of this conserved proline residue in B223 may alter the local conformation of VP4 or interactions between VP4 and VP7. The region of VP4 that includes this conserved proline has great predicted turn potential, and this is not conserved in B223 VP4. Binding of the NP1b MAbs may affect SA11 virus stability because of an effect on this proline residue, which we hypothesize may be critical for virus structure or interactions between VP4 and VP7.

The SA11 NP3 epitope 23 is the same as the RRV $3A_2$ epitope which has been localized on VP8*. The RRV $3A_2$ epitopes (amino acid substitutions at residues 87, 100, 114, and 150) were characterized by Shaw et al. (37) as RRV strain-specific MAbs except for MAb 23. Unlike the other $3A_2$ MAbs, MAb 23 possessed a low level of neutralization activity against SA11, but the site of amino acid substitution in MAb 23-selected escape mutants of RRV was not mapped. Our sequence data showed that epitope 23 was different from the other RRV $3A_2$ epitopes on SA11. Epitope 23 (aa 194) maps to the carboxyl side of the strain-specific site 5 described by Shaw and closer to the trypsin cleavage site, while the other $3A_2$ epitopes map at strain-specific sites 2, 3, and 4. The MAb 23-induced amino acid substitution is from a Tyr to a Cys (aa 194). Because the 23R mutant lost HA activity, this site may be critical for binding of virus to erythrocytes. However, because this mutant still can grow relatively well in monkey kidney cells, the HA site must not be critical for binding and replication in these cells. Assuming the binding to erythrocytes is through sialic acid, the 23R mutant may bind to MA 104 cells in a sialic acid-independent manner.

Antibodies directed to different domains of the rotavirus surface proteins reportedly neutralize virus infectivity by different neutralization mechanisms. Ruggeri and Greenberg (35) studied neutralization kinetics with VP4 (both VP8* and VP5* MAbs) and VP7 MAbs and reported that a single hit is sufficient for virus neutralization with VP7-specific MAbs but not with VP4-specific MAbs. We also examined whether single-hit kinetics could explain the neutralization of SA11 with our VP4 MAbs. We found that the ratio of antibody to epitope was at least 7.5 to 1 to obtain 93 to 99% neutralization for all of the VP4 MAbs and to effect disassembly of the virus by the NP1b MAbs. These results indicate that extensive interactions of VP4 MAb molecules with VP4 molecules on the virion are required to neutralize viral infectivity and to disassemble the viral structure by the NP1b MAbs (unpublished data). Therefore, to understand all neutralization mechanisms of rotaviruses, it is important to investigate the functional and structural domains of VP4 and VP7 and the interactions between these two proteins. The results of this study on the NP1 MAbs, together with other data on the properties of these MAbs (3), indicate that the three-dimensional folding of the native protein is such that the NP1a and NP1b subepitopes are in close proximity.

ACKNOWLEDGMENTS

This work was supported by Public Health Service grant DK 30144 from the National Institute of Diabetes and Digestive and Kidney Disease.

We thank Qing-Yi Zeng for help with the electron microscopy and Christopher Barone for help with the cell cultures.

REFERENCES

1. **Atmar, R. L., T. G. Metcalf, F. H. Neill, and M. K. Estes.** 1993. Detection of enteric viruses in oysters by using the polymerase chain reaction. Appl. Environ. Microbiol. **59:**631–635.
2. **Burns, J. W., D. Chen, M. K. Estes, and R. F. Ramig.** 1989. Biological and immunological characterization of a simian rotavirus with an altered genome segment 4. Virology **169:**427–435.
3. **Burns, J. W., H. B. Greenberg, R. D. Shaw, and M. K. Estes.** 1988. Functional and topographical analyses of epitopes on the hemagglutinin (VP4) of the simian rotavirus SA11. J. Virol. **62:**2164–2172.
4. **Caust, J., M. L. Dyall-Smith, I. Lazdins, and I. H. Homels.** 1987. Glycosylation, an important modifier of rotavirus antigenicity. Arch. Virol. **96:**123–134.
5. **Chen, D., M. K. Estes, and R. F. Ramig.** 1992. Specific interactions between rotavirus outer capsid proteins VP4 and VP7 determine expression of a cross-reactive, neutralizing VP4-specific epitope. J. Virol. **66:**432–439.
6. **Chen, D., and R. F. Ramig.** 1992. Determinants of rotavirus stability and density during CsCl purification. Virology **186:**228–237.
7. **Conner, M. E., D. O. Matson, and M. K. Estes.** 1994. Rotavirus vaccines and vaccination potential. Curr. Top. Microbiol. Immunol. **185:**253–306.
8. **Dimmock, N. J.** 1984. Mechanisms of neutralization of animal viruses. J. Gen. Virol. **65:**1015–1022.
9. **Emini, E. A., P. Ostapchuk, and E. Wimmer.** 1983. Bivalent attachment of antibody onto poliovirus leads to conformational alteration and neutralization. J. Virol. **48:**547–550.
10. **Estes, M. K., and J. Cohen.** 1989. Rotavirus gene structure and function. Microbiol. Rev. **53:**410–449.
11. **Estes, M. K., and D. Y. Graham.** 1980. Identification of rotaviruses of different origins by the plaque-reduction assay test. Am. J. Vet. Res. **41:**151–152.
12. **Estes, M. K., D. Y. Graham, and B. B. Mason.** 1981. Proteolytic enhancement of rotavirus infectivity: molecular mechanisms. J. Virol. **39:**879–888.
13. **Estes, M. K., E. L. Palmer, and J. F. Obijeski.** 1983. Rotaviruses: a review. Curr. Top. Microbiol. Immunol. **105:**123–184.
14. **Fiore, L., H. B. Greenberg, and E. R. Mackow.** 1991. The VP8 fragment of VP4 is the rhesus rotavirus hemagglutinin. Virology **181:**553–563.
15. **Gorziglia, M., G. Larralde, and R. L. Ward.** 1990. Neutralization epitopes on rotavirus SA11 4fM outer capsid proteins. J. Virol. **64:**4534–4539.
16. **Hardy, M. E., M. Gorziglia, and G. N. Woode.** 1992. Amino acid sequence analysis of bovine rotavirus B223 reveals a unique outer capsid protein VP4 and confirms a third bovine VP4 type. Virology **191:**291–300.
17. **Hoshino, Y., M. M. Sereno, K. Midthun, J. Flores, A. Z. Kapikian, and R. M. Chanock.** 1985. Independent segregation of two antigenic specificities (VP3 and VP7) involved in neutralization of rotavirus infectivity. Proc. Natl. Acad. Sci. USA **82:**8701–8704.
18. **Jiang, X., M. Wang, D. Y. Graham, and M. K. Estes.** 1992. Expression, self-assembly, and antigenicity of the Norwalk virus capsid protein. J. Virol. **66:**6527–6532.
19. **Kapikian, A. Z., and R. M. Chanock.** 1990. Rotaviruses, p. 1353–1404. *In* B. N. Fields and D. M. Knipe (ed.), Virology. Raven Press, New York.
20. **Lizano, M., S. López, and C. F. Arias.** 1991. The amino-terminal half of rotavirus SA114fM VP4 protein contains a hemagglutination domain and primes for neutralizing antibodies to the virus. J. Virol. **65:**1383–1391.
21. **López, S., I. López, P. Romero, E. Méndez, X. Soberón, and C. F. Arias.** 1991. Rotavirus YM gene 4: analysis of its deduced amino acid sequence and prediction of the secondary structure of the VP4 protein. J. Virol. **65:**3738–3745.
22. **Lubeck, M. D., and W. Gerhard.** 1981. Topological mapping of the antigenic sites on the influenza A/PR/8/34 virus hemagglutinin using monoclonal antibodies. Virology **113:**64–72.
23. **Mackow, E. R., R. D. Shaw, S. M. Matsui, P. T. Vo, M. N. Ngoc, and H. B. Greenberg.** 1988. The rhesus rotavirus gene encoding VP3: location of amino acids involved in homologous and heterologous rotavirus neutralization and identification of a putative fusion region. Proc. Natl. Acad. Sci. USA **85:**645–649.
24. **Mackow, E. R., R. D. Shaw, S. M. Matsui, P. T. Vo, D. A. Benfield, and H. B. Greenberg.** 1988. Characterization of

homotypic and heterotypic VP7 neutralization sites of rhesus rotavirus. Virology **165:**511–517.

25. **Matsui, S. M., E. R. Mackow, and H. B. Greenberg.** 1989. Molecular determinant of rotavirus neutralization and protection. Adv. Virus Res. **36:**181–214.
26. **Matsui, S. M., P. A. Offit, P. T. Vo, E. R. Mackow, D. A. Benfield, R. D. Shaw, L. Padilla-Noriega, and H. B. Greenberg.** 1989. Passive protection against rotavirus-induced diarrhea by monoclonal antibodies to the heterotypic neutralization domain of VP7 and the VP8 fragment of VP4. J. Clin. Microbiol. **27:**780–782.
27. **Mattion, N. M., J. Cohen, and M. K. Estes.** 1993. Rotavirus proteins, p. 169–249. *In* A. Z. Kapikian (ed.), Viral infections of the gastrointestinal tract. Marcel Dekker, Inc., New York.
28. **Mattion, N. M., and M. K. Estes.** 1991. Sequence of a rotavirus gene 4 associated with unique biologic properties. Arch. Virol. **120:**109–113.
29. **McCullough, K. C., C. J. Smale, W. C. Carpenter, J. R. Crowther, E. Broucchi, and F. D. Simone.** 1987. Conformational alteration in foot-and-mouth disease virus virion capsid structure after complexing with monospecific antibody. Immunology **60:**75–82.
30. **Offit, P. A., and G. Blavat.** 1986. Identification of the two rotavirus genes determining neutralization specificities. J. Virol. **57:**376–378.
31. **Offit, P. A., H. F. Clark, G. Blavat, and H. B. Greenberg.** 1986. Reassortant rotaviruses containing structural proteins vp3 and vp7 from different parents induce antibodies protective against each parental serotype. J. Virol. **60:**491–496.
32. **Offit, P. A., R. D. Shaw, and H. B. Greenberg.** 1986. Passive protection against rotavirus-induced diarrhea by monoclonal antibodies to surface proteins vp3 and vp7. J. Virol. **58:**700–703.
33. **Prasad, B. V. V., J. W. Burns, E. Marietta, M. K. Estes, and W. Chiu.** 1990. Localization of VP4 neutralization sites in rotavirus by three-dimensional cryo-electron microscopy. Nature (London) **343:**476–479.
34. **Prasad, B. V. V., G. J. Wang, J. P. M. Clerx, and W. Chiu.** 1988. Three dimensional structure of rotavirus. J. Mol. Biol. **199:**269–275.
35. **Ruggeri, F. M., and H. B. Greenberg.** 1991. Antibodies to the trypsin cleavage peptide VP8* neutralize rotavirus by inhibiting binding of virions to target cells in culture. J. Virol. **65:**2211–2219.
36. **Shaw, A. L., R. Rothnagel, D. Chen, R. F. Ramig, W. Chiu, and B. V. V. Prasad.** 1993. Three-dimensional visualization of the rotavirus hemagglutinin structure. Cell **74:**693–701.
37. **Shaw, R. D., P. T. Vo, P. A. Offit, B. S. Coulson, and H. B. Greenberg.** 1986. Antigenic mapping of the surface proteins of rhesus rotavirus. Virology **155:**434–451.
38. **Taniguchi, K., Y. Hoshino, K. Nishikawa, K. Y. Green, W. L. Maloy, Y. Morita, S. Urasawa, A. Z. Kapikian, R. M. Chanock, and M. Gorziglia.** 1988. Cross-reactive and serotype-specific neutralization epitopes on VP7 of human rotavirus: nucleotide sequence analysis of antigenic mutants selected with monoclonal antibodies. J. Virol. **62:**1870–1874.
39. **Taniguchi, K., W. L. Maloy, K. Nishikawa, K. Y. Green, Y. Hoshino, S. Urasawa, A. Z. Kapikian, R. M. Chanock, and M. Gorziglia.** 1988. Identification of cross-reactive and serotype 2-specific neutralization epitopes on VP3 of human rotavirus. J. Virol. **62:**2421–2426.
40. **Taniguchi, K., Y. Morita, T. Urasawa, and S. Urasawa.** 1987. Cross-reactive neutralization epitopes on VP3 of human rotavirus: analysis with monoclonal antibodies and antigenic variants. J. Virol. **61:**1726–1730.
41. **Wohlfart, C.** 1988. Neutralization of adenovirus: kinetics, stoichiometry, and mechanisms. J. Virol. **62:**2321–2328.